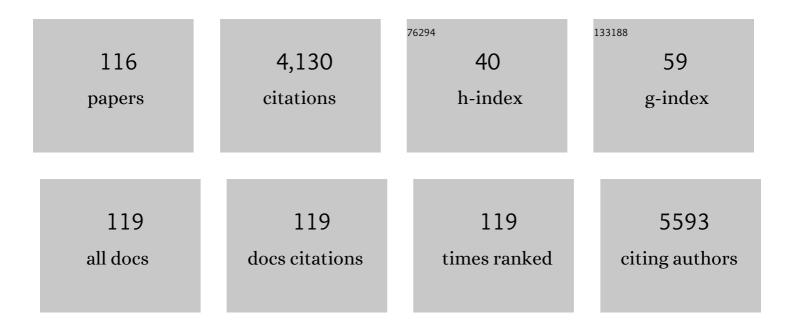
List of Publications by Year in descending order

Source: https://exaly.com/author-pdf/5189713/publications.pdf Version: 2024-02-01



#	Article	IF	CITATIONS
1	Full-view in vivo skin and blood vessels profile segmentation in photoacoustic imaging based on deep learning. Photoacoustics, 2022, 25, 100310.	4.4	15
2	Enhanced precision of real-time control photothermal therapy using cost-effective infrared sensor array and artificial neural network. Computers in Biology and Medicine, 2022, 141, 104960.	3.9	3
3	The impact of Cu(II) ions doping in nanostructured hydroxyapatite powder: A finite element modelling study for physico-mechanical and biological property evaluation. Advanced Powder Technology, 2022, 33, 103405.	2.0	11
4	A Flexible, Wearable, and Wireless Biosensor Patch with Internet of Medical Things Applications. Biosensors, 2022, 12, 139.	2.3	32
5	Computational analysis of drug free silver triangular nanoprism theranostic probe plasmonic behavior for in-situ tumor imaging and photothermal therapy. Journal of Advanced Research, 2022, 41, 23-38.	4.4	11
6	Fluorescence conjugated nanostructured cobalt-doped hydroxyapatite platform for imaging-guided drug delivery application. Colloids and Surfaces B: Biointerfaces, 2022, 214, 112458.	2.5	10
7	Design and Micro-Fabrication of Focused High-Frequency Needle Transducers for Medical Imaging. Sensors, 2022, 22, 3763.	2.1	1
8	Smart inexpensive quantitative urine glucose and contaminant bromide ion sensor based on metal nanoparticles with deep learning approach. Materials Chemistry and Physics, 2022, 287, 126289.	2.0	2
9	Development of Scanning Acoustic Microscopy System for Evaluating the Resistance Spot Welding Quality. Research in Nondestructive Evaluation, 2022, 33, 123-137.	0.5	2
10	Development of fast photoacoustic and ultrasound imaging system based on slider-crank scanner for small animals and humans study. Expert Systems With Applications, 2022, 206, 117939.	4.4	4
11	Recent Progress on Nanostructured Materials for Biomedical Applications. Environmental and Microbial Biotechnology, 2021, , 349-373.	0.4	0
12	Design of a nearly linear-phase IIR filter and JPEG compression ECG signal in real-time system. Biomedical Signal Processing and Control, 2021, 67, 102431.	3.5	9
13	Design of a High-Power Multilevel Sinusoidal Signal and High-Frequency Excitation Module Based on FPGA for HIFU Systems. Electronics (Switzerland), 2021, 10, 1299.	1.8	2
14	Rice starch coated iron oxide nanoparticles: A theranostic probe for photoacoustic imaging-guided photothermal cancer therapy. International Journal of Biological Macromolecules, 2021, 183, 55-67.	3.6	23
15	Fluorescence/photoacoustic imaging-guided nanomaterials for highly efficient cancer theragnostic agent. Scientific Reports, 2021, 11, 15943.	1.6	17
16	A smart LED therapy device with an automatic facial acne vulgaris diagnosis based on deep learning and internet of things application. Computers in Biology and Medicine, 2021, 136, 104610.	3.9	16
17	Ultra-widefield photoacoustic microscopy with a dual-channel slider-crank laser-scanning apparatus for in vivo biomedical study. Photoacoustics, 2021, 23, 100274.	4.4	10
18	A flexible, and wireless LED therapy patch for skin wound photomedicine with IoT-connected healthcare application. Flexible and Printed Electronics, 2021, 6, 045002.	1.5	10

#	Article	IF	CITATIONS
19	Roles of Chitosan in Green Synthesis of Metal Nanoparticles for Biomedical Applications. Nanomaterials, 2021, 11, 273.	1.9	52
20	Hydroxyapatite nano bioceramics optimized 3D printed poly lactic acid scaffold for bone tissue engineering application. Ceramics International, 2020, 46, 3443-3455.	2.3	128
21	Fabrication and biological activity of polycaprolactone/phlorotannin endotracheal tube to prevent tracheal stenosis: An in vitro and in vivo study. Journal of Biomedical Materials Research - Part B Applied Biomaterials, 2020, 108, 1046-1056.	1.6	17
22	Folic acid–conjugated chitosan-functionalized graphene oxide for highly efficient photoacoustic imaging-guided tumor-targeted photothermal therapy. International Journal of Biological Macromolecules, 2020, 155, 961-971.	3.6	60
23	Chitosan and their derivatives: Antibiofilm drugs against pathogenic bacteria. Colloids and Surfaces B: Biointerfaces, 2020, 185, 110627.	2.5	139
24	An Up-To-Date Review on Biomedical Applications of Palladium Nanoparticles. Nanomaterials, 2020, 10, 66.	1.9	98
25	A portable device with low-power consumption for monitoring mouse vital signs during in vivo photoacoustic imaging and photothermal therapy. Physiological Measurement, 2020, 41, 125011.	1.2	6
26	Fuzzy Logic Control-Based HIFU System Integrated with Photoacoustic Imaging Module for Ex Vivo Artificial Tumor Treatment. Applied Sciences (Switzerland), 2020, 10, 7888.	1.3	7
27	Rare earth element doped hydroxyapatite luminescent bioceramics contrast agent for enhanced biomedical imaging and therapeutic applications. Ceramics International, 2020, 46, 29249-29260.	2.3	35
28	Design of a Multichannel Pulser/Receiver and Optimized Damping Resistor for High-Frequency Transducer Applied to SAM System. Applied Sciences (Switzerland), 2020, 10, 8388.	1.3	2
29	Development of a LED light therapy device with power density control using a Fuzzy logic controller. Medical Engineering and Physics, 2020, 86, 71-77.	0.8	10
30	Real-Time Filtering and ECG Signal Processing Based on Dual-Core Digital Signal Controller System. IEEE Sensors Journal, 2020, 20, 6492-6503.	2.4	20
31	Improved Depth-of-Field Photoacoustic Microscopy with a Multifocal Point Transducer for Biomedical Imaging. Sensors, 2020, 20, 2020.	2.1	13
32	Fabrication of High Frequency Transducer for Nondestructive Testing. Journal of Power System Engineering, 2020, 24, 36-42.	0.4	1
33	Chitosan oligosaccharide coated mesoporous silica nanoparticles for pH-stimuli responsive drug delivery applications. Journal of Porous Materials, 2019, 26, 217-226.	1.3	25
34	Anti-EGFR antibody conjugated thiol chitosan-layered gold nanoshells for dual-modal imaging-guided cancer combination therapy. Journal of Controlled Release, 2019, 311-312, 26-42.	4.8	55
35	Indocyanine green and poly I:C containingÂthermo-responsive liposomes used in immune-photothermal therapy prevent cancer growth and metastasis. , 2019, 7, 220.		57
36	Synthesis and characterization of chitosan oligosaccharide-capped gold nanoparticles as an effective antibiofilm drug against the Pseudomonas aeruginosa PAO1. Microbial Pathogenesis, 2019, 135, 103623.	1.3	51

#	Article	IF	CITATIONS
37	Biofilm inhibition, modulation of virulence and motility properties by FeOOH nanoparticle in Pseudomonas aeruginosa. Brazilian Journal of Microbiology, 2019, 50, 791-805.	0.8	29
38	Photothermal Responsive Porous Membrane for Treatment of Infected Wound. Polymers, 2019, 11, 1679.	2.0	22
39	Thiol chitosan-wrapped gold nanoshells for near-infrared laser-induced photothermal destruction of antibiotic-resistant bacteria. Carbohydrate Polymers, 2019, 225, 115228.	5.1	50
40	A multifunctional near-infrared laser-triggered drug delivery system using folic acid conjugated chitosan oligosaccharide encapsulated gold nanorods for targeted chemo-photothermal therapy. Journal of Materials Chemistry B, 2019, 7, 3811-3825.	2.9	40
41	Design, Fabrication, and Evaluation of Multifocal Point Transducer for High-Frequency Ultrasound Applications. Sensors, 2019, 19, 609.	2.1	4
42	Antibiofilm and antivirulence properties of chitosan-polypyrrole nanocomposites to Pseudomonas aeruginosa. Microbial Pathogenesis, 2019, 128, 363-373.	1.3	47
43	Nanostructured hollow hydroxyapatite fabrication by carbon templating for enhanced drug delivery and biomedical applications. Ceramics International, 2019, 45, 17081-17093.	2.3	40
44	Chitosan-mediated facile green synthesis of size-controllable gold nanostars for effective photothermal therapy and photoacoustic imaging. European Polymer Journal, 2019, 118, 492-501.	2.6	29
45	Enhanced rheological behaviors of alginate hydrogels with carrageenan for extrusion-based bioprinting. Journal of the Mechanical Behavior of Biomedical Materials, 2019, 98, 187-194.	1.5	122
46	Design of a Solar-Powered Portable ECG Device with Optimal Power Consumption and High Accuracy Measurement. Applied Sciences (Switzerland), 2019, 9, 2129.	1.3	10
47	Fucoidan-Stabilized Gold Nanoparticle-Mediated Biofilm Inhibition, Attenuation of Virulence and Motility Properties in Pseudomonas aeruginosa PAO1. Marine Drugs, 2019, 17, 208.	2.2	71
48	Comparative characterization of biogenic and chemical synthesized hydroxyapatite biomaterials for potential biomedical application. Materials Chemistry and Physics, 2019, 228, 344-356.	2.0	58
49	The Reference Phase Correction for the Fluctuated Scanning Lines and the Slope of the Stage in Tissue Characterization by Scanning Acoustic Microscope. Applied Sciences (Switzerland), 2019, 9, 4883.	1.3	Ο
50	Chitosan/fucoidan multilayer coating of gold nanorods as highly efficient near-infrared photothermal agents for cancer therapy. Carbohydrate Polymers, 2019, 211, 360-369.	5.1	68
51	Photoacoustic Monitoring of the Viability of Mesenchymal Stem Cells Labeled with Indocyanine Green. Irbm, 2019, 40, 45-50.	3.7	4
52	Rapid microwave-assisted synthesis of gold loaded hydroxyapatite collagen nano-bio materials for drug delivery and tissue engineering application. Ceramics International, 2019, 45, 2977-2988.	2.3	61
53	Nanostructured Materials and Their Biomedical Application. , 2019, , 205-227.		1
54	Fish bone peptide promotes osteogenic differentiation of MC3T3â€E1 preâ€osteoblasts through upregulation of MAPKs and Smad pathways activated BMPâ€2 receptor. Cell Biochemistry and Function, 2018, 36, 137-146.	1.4	48

#	Article	IF	CITATIONS
55	In vivo photoacoustic monitoring using 700-nm region Raman source for targeting Prussian blue nanoparticles in mouse tumor model. Scientific Reports, 2018, 8, 2000.	1.6	23
56	Optimized Zn-doped hydroxyapatite/doxorubicin bioceramics system for efficient drug delivery and tissue engineering application. Ceramics International, 2018, 44, 6062-6071.	2.3	89
57	Multimodal tumor-homing chitosan oligosaccharide-coated biocompatible palladium nanoparticles for photo-based imaging and therapy. Scientific Reports, 2018, 8, 500.	1.6	102
58	Synthesis of urea-pyridyl ligand functionalized mesoporous silica hybrid material for hydrophobic and hydrophilic drug delivery application. Journal of Porous Materials, 2018, 25, 119-128.	1.3	5
59	Photo-based PDT/PTT dual model killing and imaging of cancer cells using phycocyanin-polypyrrole nanoparticles. European Journal of Pharmaceutics and Biopharmaceutics, 2018, 123, 20-30.	2.0	53
60	Marine natural pigments as potential sources for therapeutic applications. Critical Reviews in Biotechnology, 2018, 38, 745-761.	5.1	69
61	Fucoidan-coated CuS nanoparticles for chemo-and photothermal therapy against cancer. Oncotarget, 2018, 9, 12649-12661.	0.8	48
62	Immunostimulatory Agent Evaluation: Lymphoid Tissue Extraction and Injection Route-Dependent Dendritic Cell Activation. Journal of Visualized Experiments, 2018, , .	0.2	1
63	Biocompatible sphere, square prism and hexagonal rod Gd2O3:Eu3+@SiO2 nanoparticles: The effect of morphology on multi-modal imaging. Colloids and Surfaces B: Biointerfaces, 2018, 172, 224-232.	2.5	8
64	Nano-hydroxyapatite bioactive glass composite scaffold with enhanced mechanical and biological performance for tissue engineering application. Ceramics International, 2018, 44, 15735-15746.	2.3	65
65	Biomimetic synthesis of metal–hydroxyapatite (Au-HAp, Ag-HAp, Au-Ag-HAp): Structural analysis, spectroscopic characterization and biomedical application. Ceramics International, 2018, 44, 20490-20500.	2.3	64
66	Biocompatible Chitosan Oligosaccharide Modified Gold Nanorods as Highly Effective Photothermal Agents for Ablation of Breast Cancer Cells. Polymers, 2018, 10, 232.	2.0	39
67	Coating Chitosan Thin Shells: A Facile Technique to Improve Dispersion Stability of Magnetoliposomes. Journal of Nanoscience and Nanotechnology, 2018, 18, 583-590.	0.9	6
68	Photoacoustic Imaging-Guided Photothermal Therapy with Tumor-Targeting HA-FeOOH@PPy Nanorods. Scientific Reports, 2018, 8, 8809.	1.6	53
69	Synthesis of Fe3O4 modified mesoporous silica hybrid for pH-responsive drug delivery and magnetic hyperthermia applications. Journal of Porous Materials, 2018, 25, 1251-1264.	1.3	15
70	Feasibility of photoacoustic evaluations on dualâ€ŧhermal treatment of <i>ex vivo</i> bladder tumors. Journal of Biophotonics, 2017, 10, 577-588.	1.1	13
71	Photothermal-triggered control of sub-cellular drug accumulation using doxorubicin-loaded single-walled carbon nanotubes for the effective killing of human breast cancer cells. Nanotechnology, 2017, 28, 125101.	1.3	37
72	Multifunctional biocompatible chitosan-polypyrrole nanocomposites as novel agents for photoacoustic imaging-guided photothermal ablation of cancer. Scientific Reports, 2017, 7, 43593.	1.6	75

#	Article	IF	CITATIONS
73	Anti-EGFR Antibody Conjugation of Fucoidan-Coated Gold Nanorods as Novel Photothermal Ablation Agents for Cancer Therapy. ACS Applied Materials & Interfaces, 2017, 9, 14633-14646.	4.0	55
74	Chlorin e6 conjugated copper sulfide nanoparticles for photodynamic combined photothermal therapy. Photodiagnosis and Photodynamic Therapy, 2017, 19, 128-134.	1.3	37
75	Marine Biopolymer-Based Nanomaterials as a Novel Platform for Theranostic Applications. Polymer Reviews, 2017, 57, 631-667.	5.3	45
76	Magnetic hyperthermia and pH-responsive effective drug delivery to the sub-cellular level of human breast cancer cells by modified CoFe2O4 nanoparticles. Biochimie, 2017, 133, 7-19.	1.3	63
77	Making unpolarized light sensitive to polarization-sensitive devices. Applied Physics B: Lasers and Optics, 2017, 123, 1.	1.1	0
78	Ex vivodetection of macrophages in atherosclerotic plaques using intravascular ultrasonic-photoacoustic imaging. Physics in Medicine and Biology, 2017, 62, 501-516.	1.6	7
79	Rabbit model of tracheal stenosis using cylindrical diffuser. Lasers in Surgery and Medicine, 2017, 49, 372-379.	1.1	10
80	Astaxanthin conjugated polypyrrole nanoparticles as a multimodal agent for photo-based therapy and imaging. International Journal of Pharmaceutics, 2017, 517, 216-225.	2.6	31
81	Crown ether triad modified core–shell magnetic mesoporous silica nanocarrier for pH-responsive drug delivery and magnetic hyperthermia applications. New Journal of Chemistry, 2017, 41, 10935-10947.	1.4	18
82	Subcellular domain-dependent molecular hierarchy of SFK and FAK in mechanotransduction and cytokine signaling. Scientific Reports, 2017, 7, 9033.	1.6	10
83	Synthesis of surface capped mesoporous silica nanoparticles for pH-stimuli responsive drug delivery applications. MedChemComm, 2017, 8, 1797-1805.	3.5	19
84	Polypyrrole–methylene blue nanoparticles as a single multifunctional nanoplatform for near-infrared photo-induced therapy and photoacoustic imaging. RSC Advances, 2017, 7, 35027-35037.	1.7	39
85	Synthesis and In Vitro Performance of Polypyrrole-Coated Iron–Platinum Nanoparticles for Photothermal Therapy and Photoacoustic Imaging. Nanoscale Research Letters, 2017, 12, 570.	3.1	34
86	Fucoidan-coated core–shell magnetic mesoporous silica nanoparticles for chemotherapy and magnetic hyperthermia-based thermal therapy applications. New Journal of Chemistry, 2017, 41, 15334-15346.	1.4	39
87	Biocompatible astaxanthin as novel contrast agent for biomedical imaging. Journal of Biophotonics, 2017, 10, 1053-1061.	1.1	16
88	Doxorubicin-fucoidan-gold nanoparticles composite for dual-chemo-photothermal treatment on eye tumors. Oncotarget, 2017, 8, 113719-113733.	0.8	44
89	Magnetic hydroxyapatite: a promising multifunctional platform for nanomedicine application. International Journal of Nanomedicine, 2017, Volume 12, 8389-8410.	3.3	79
90	Synergistic Antibacterial Effects of Chitosan-Caffeic Acid Conjugate against Antibiotic-Resistant Acne-Related Bacteria. Marine Drugs, 2017, 15, 167.	2.2	60

#	Article	IF	CITATIONS
91	Hydroxyapatite Coated Iron Oxide Nanoparticles: A Promising Nanomaterial for Magnetic Hyperthermia Cancer Treatment. Nanomaterials, 2017, 7, 426.	1.9	105
92	Polarimetric Fiber Vibration Sensor Based on Polarization-Diversified Loop Using Short Polarization-Maintaining Photonic Crystal Fiber. Journal of Nanoscience and Nanotechnology, 2017, 17, 8307-8312.	0.9	2
93	Chlorin e6 conjugated silica nanoparticles for targeted and effective photodynamic therapy. Photodiagnosis and Photodynamic Therapy, 2017, 19, 212-220.	1.3	63
94	Laminarin promotes anti-cancer immunity by the maturation of dendritic cells. Oncotarget, 2017, 8, 38554-38567.	0.8	45
95	Lipopolysaccharide-coated CuS nanoparticles promoted anti-cancer and anti-metastatic effect by immuno-photothermal therapy. Oncotarget, 2017, 8, 105584-105595.	0.8	24
96	Cytotoxic Induction and Photoacoustic Imaging of Breast Cancer Cells Using Astaxanthin-Reduced Gold Nanoparticles. Nanomaterials, 2016, 6, 78.	1.9	25
97	Effect of multipleâ€sweeping on ablation performance during <i>ex vivo</i> laser nephrectomy. Lasers in Surgery and Medicine, 2016, 48, 616-623.	1.1	4
98	MAGE-A1–6 expression in patients with head and neck squamous cell carcinoma: impact on clinical patterns and oncologic outcomes. International Journal of Clinical Oncology, 2016, 21, 875-882.	1.0	10
99	Theoretical development of a magnetic force and an induced motion in elastic media for a magneto-motive technique. Journal of the Korean Physical Society, 2016, 69, 461-471.	0.3	2
100	Synthesis of amine-polyglycidol functionalised Fe ₃ O ₄ @SiO ₂ nanocomposites for magnetic hyperthermia, pH-responsive drug delivery, and bioimaging applications. RSC Advances, 2016, 6, 110444-110453.	1.7	34
101	Paclitaxel-loaded chitosan oligosaccharide-stabilized gold nanoparticles as novel agents for drug delivery and photoacoustic imaging of cancer cells. International Journal of Pharmaceutics, 2016, 511, 367-379.	2.6	110
102	Doxorubicin-loaded fucoidan capped gold nanoparticles for drug delivery and photoacoustic imaging. International Journal of Biological Macromolecules, 2016, 91, 578-588.	3.6	149
103	Fabrication, characterization and determination of biological activities of poly(ε-caprolactone)/chitosan-caffeic acid composite fibrous mat for wound dressing application. International Journal of Biological Macromolecules, 2016, 93, 1549-1558.	3.6	43
104	Bidirectional laser triggering in highly-resistive vanadium-dioxide thin films by using a 966-nm pump laser diode. Journal of the Korean Physical Society, 2016, 68, 323-328.	0.3	4
105	Anti-allergic effects of a nonameric peptide isolated from the intestine gastrointestinal digests of abalone (Haliotis discus hannai) in activated HMC-1 human mast cells. International Journal of Molecular Medicine, 2016, 37, 243-250.	1.8	16
106	Marine microorganisms as potential biofactories for synthesis of metallic nanoparticles. Critical Reviews in Microbiology, 2016, 42, 1007-1019.	2.7	80
107	Marine polysaccharide-based nanomaterials as a novel source of nanobiotechnological applications. International Journal of Biological Macromolecules, 2016, 82, 315-327.	3.6	158
108	Production of a Novel Fucoidanase for the Green Synthesis of Gold Nanoparticles by Streptomyces sp. and Its Cytotoxic Effect on HeLa Cells. Marine Drugs, 2015, 13, 6818-6837.	2.2	52

JUNGHWAN OH

#	Article	IF	CITATIONS
109	Intravascular ultrasonic–photoacoustic (IVUP) endoscope with 2.2-mm diameter catheter for medical imaging. Computerized Medical Imaging and Graphics, 2015, 45, 57-62.	3.5	19
110	Enhancement of high-resolution photoacoustic imaging with indocyanine green-conjugated carbon nanotubes. Japanese Journal of Applied Physics, 2015, 54, 07HF04.	0.8	14
111	Memristive states in vanadium-dioxide-based planar devices stimulated by 966 nm infrared laser pulses. Japanese Journal of Applied Physics, 2015, 54, 102601.	0.8	6
112	Thermoelastic displacement measured by DP-OCT for detecting vulnerable plaques. Biomedical Optics Express, 2014, 5, 474.	1.5	2
113	Feasibility study on photoacoustic guidance for high-intensity focused ultrasound-induced hemostasis. Journal of Biomedical Optics, 2014, 19, 105010.	1.4	17
114	<i>In vivo</i> non-ionizing photoacoustic mapping of sentinel lymph nodes and bladders with ICG-enhanced carbon nanotubes. Physics in Medicine and Biology, 2012, 57, 7853-7862.	1.6	79
115	Controlling the optimum dose of AMPTS functionalized-magnetite nanoparticles for hyperthermia cancer therapy. Applied Nanoscience (Switzerland), 2011, 1, 237-246.	1.6	23
116	Inline Conversion Between Transmission and Reflection Spectra of Fiber Bragg Grating Using Polarization-Diversity Loop Structure. IEEE Photonics Technology Letters, 2010, 22, 1473-1475.	1.3	6